JOURNAL OF AIRCRAFT
Vol. 31, No. 3, May–June 1994

# Comprehensive Model of Anisotropic Composite Aircraft Wings Suitable for Aeroelastic Analyses

G. Karpouzian*
*U.S. Naval Academy, Annapolis, Maryland 21402*
and
L. Librescu†
*Virginia Polytechnic Institute and State University, Blacksburg, Virginia 24061*

**A comprehensive plate-beam structural model suitable for aeroelastic analyses of aircraft wings made of anisotropic composite materials is developed. The equations governing the static and dynamic aeroelastic equilibrium of cantilevered swept-wing structures and the associated boundary conditions are derived by means of the Hamilton variational principle. These equations incorporate a number of effects: 1) anisotropy of the materials of constituent layers, 2) warping inhibition, 3) transverse shear flexibility, and 4) rotatory inertias. A uniform swept-wing model composed of a transversely isotropic material is considered to illustrate the coupled and separate effects of transverse shear deformation and warping restraint upon its divergence and static aeroelastic load distribution. An exact method based upon the Laplace integral transform technique is used to solve the above mentioned problems. The results displayed in this article reveal the importance of transverse shear and warping restraint effects in predicting more accurately the static aeroelastic response of swept-forward wings. However, for swept-back wings, these effects represent higher-order corrections to the classical theory.**

## Nomenclature

| | | |
|---|---|---|
| AR | = | wing aspect ratio |
| $a_0$ | = | sectional lift-curve slope |
| $C_{mac}$ | = | sectional pitching moment coefficient about the aerodynamic center (positive nose up) |
| $c$ | = | wing chord length measured perpendicular to the reference axis |
| $d$, $\bar{d}$ | = | offset between the line of c.m. and the elastic axis (positive forward), $d/c$ |
| $E$ | = | Young's modulus |
| $e$, $\bar{e}$ | = | offset between the spanwise reference axis and aerodynamic centerline (positive forward), $e/c$ |
| $G'$ | = | transverse shear modulus |
| $h$ | = | plunging displacement, positive upward |
| $H$, $\bar{H}$ | = | thickness of wing cross section, $H/c$ |
| $\mathcal{L}$ | = | sectional lift, positive upward |
| $LT$ | = | Laplace transform operator |
| $l$ | = | wing semispan measured along the reference axis |
| $N$ | = | load factor normal to the wing surface |
| $P$ | = | static pressure |
| $Q_n$, $Q_n^*$, $\bar{Q}_n$ | = | nondimensional dynamic pressure $\equiv q_n c l^3/\bar{D}_{22}$, nondimensional divergence pressure corresponding to $E/G' = 0$, $Q_n/Q_n^*$ |
| $q_n$ | = | component of the dynamic pressure normal to the reference axis, $\equiv \rho V_n^2/2$ |
| $R$ | = | transverse shear flexibility parameter, $E/G'$ |
| $s$ | = | complex variable for Laplace transformation |
| $\mathcal{T}$ | = | sectional aerodynamic torque about the elastic axis, positive nose up |
| $V_n$ | = | component of the freestream velocity normal to the reference axis |
| $W$ | = | aircraft weight |
| $x_1$, $x_2$, $x_3$ | = | chordwise, spanwise, and transverse normal coordinate to the midplane of the wing, respectively |
| $\alpha_0$ | = | prescribed rigid wing angle of attack |
| $\delta_1$ | = | tracer, taken as 1 for warping restraint and 0 for free warping |
| $\eta$ | = | $x_2/l$ |
| $\theta$ | = | twist angle |
| $\Lambda$ | = | sweep angle of the reference axis (positive for swept back) |
| $\nu$ | = | Poisson's ratio |
| $\psi_1$, $\psi_2$ | = | angles of rotation of a line element originally normal to the reference plane, about the $x_2$ and $x_1$ axes, respectively |
| $\cup$ | = | reunion sign |
| $(\ )_{,2}$, $(\ )'$ | = | $\mathrm{d}(\ )/\mathrm{d}x_2$, $\mathrm{d}(\ )/\mathrm{d}\eta$ |

Presented as Paper 91-0934 at the AIAA/ASME/ASCE/AHS/ASC 32nd Structures, Structural Dynamics and Materials Conference, Baltimore, MD, April 8–10, 1991; received Aug. 28, 1992; revision received April 8, 1993; accepted for publication, April 8, 1993. 

*Associate Professor, Aerospace Engineering Department.
†Professor, Engineering Science and Mechanics Department.

## Introduction

OVER the last two decades advanced composite materials have been increasingly used in the design of aircraft and spacecraft to decrease their weight, increase performance, and allow the development of novel structural configurations. Due to their outstanding properties, the advanced composite materials are prime candidates for the design of the next generation of aeronautical and aerospace vehicles.

Their unique features, manifested in terms of their anisotropy, structural couplings, transverse shear flexibility, etc., require a better understanding of their implications in aeroelastic analyses. To this end, the structural models used so far to study the aeroelastic behavior of metallic wing structures have to be modified to include the new effects which are prominent for the composite structures.

Within an earlier stage of the research activity, started only 15 yr ago, the classical equations governing the motion of metallic wing structures have been extended to incorporate the anisotropy and heterogeneity properties. These studies prompted by Krone[1] and Weisshaar[2–5] and followed by other aeroelasticians[6–11] have revealed the following:

1) The wing structures made of anisotropic composite materials can be tailored to improve their aeroelastic response characteristics.

2) The application of this technology can result in the elimination of the divergence instability, a chronic problem facing the aeroelastic behavior of swept-forward wing airplane.

Another degree of refinement consists of the incorporation of the warping restraint effect. The study of its implications on the static aeroelastic problems of swept-forward composite anisotropic wing aircraft was accomplished.[12-15]

The results concerning the structural[16-20] and aeroelastic[12-15] behavior of cantilevered structures fully reveal that, in the case of composite materials, the effect of warping inhibition becomes more prominent and more complex than in the case of their metallic counterparts.[21] As was shown in Refs. 13–15, due to elastic couplings featuring the composite cantilevered structures, the restraint of warping could yield not only an increase of the divergence speed, as it was the case for metallic wing structures,[21] but also a decrease of it even for high aspect ratio wings.

In addition to the above mentioned effects, the composite material structures exhibit large flexibilities in transverse shear, contradicting the usual assumption of infinite rigidity postulated by the classical theory.[22] Inherent to composite materials, this transverse shear flexibility could result in severe detrimental effects upon the aeroelastic behavior of aircraft structures. Moreover, during the high-speed flight regimes, or during the entry or re-entry into the terrestrial atmosphere, due to the high temperature fields induced by large heat-transfer rates from high-speed flows to the vehicle structure, this transverse shear flexibility could increase further.

Inclusion of these effects into the aeroelastic analysis could result in corrections of order of magnitude comparable to or even higher than the results obtained by classical theories. These drastic changes cannot be ignored or underestimated, and as a result, for an improved prediction of aeroelastic behavior of wing structures composed of advanced composite materials, this shear flexibility should be incorporated.

As a first step, the equations governing the aeroelastic equilibrium of cantilevered wing structures made of anisotropic composite materials and incorporating the various elastic and structural couplings, the warping restraint, and transverse shear effect will be established. An application of the present theory to the study of divergence and aeroelastic load distribution of swept-wing structures constructed of transversely isotropic material will be presented. The combined and separate effects of warping restraint (WR), free warping (FW), and transverse shear deformation (TSD) on the static aeroelastic response will be evaluated and discussed.

## Basic Assumptions

The concept of shear deformable plate-beam model will be adopted. The wing structure is idealized as a laminated composite plate whose constituent laminae are characterized by different orthotropicity angles and different material and thickness properties. Let $n$ be the total number of constituent layers. The interface plane between the contiguous layers $r$ and $r + 1$ ($1 \leq r \leq n$) will be selected as the reference plane of the composite structure. The points of the reference of the wing (defined by $x_3 = 0$) are referred to a Cartesian system of in-plane coordinates $(x_1, x_2)$; the upward $x_3$ coordinate being considered perpendicular to the $(x_1, x_2)$ plane. The chordwise location of the $x_2$ coordinate is as yet unspecified.

We also postulate the chordwise nondeformability of the wing structure. This assumption is justified by the fact that the semimonocoque wing structures usually contain transverse stiffening members which are rigid within their own planes.

## Kinematic Equations

To the end of obtaining the kinematic relations, the following representation for the displacement components of the three-dimensional body of the structure will be used:

$$U_1(x_1, x_2, x_3; t) = u_1(x_1, x_2; t) + x_3\psi_1(x_1, x_2; t) \quad (1a)$$

$$U_2(x_1, x_2, x_3; t) = u_2(x_1, x_2; t) + x_3\psi_2(x_1, x_2; t) \quad (1b)$$

$$U_3(x_1, x_2, x_3; t) = u_3(x_1, x_2; t) \quad (1c)$$

Here $(u_1, u_2, u_3)$ denote the displacement components along $(x_1, x_2, x_3)$ coordinates and are associated with the points of the reference plane of the composite panel ($x_3 = 0$); $t$ denotes the time variable. Equation (1) corresponds to the first-order transverse shear deformation theory (FSDT) (see e.g., Refs. 22 and 23).

Consistent with the chordwise-rigid plate model, we may consider that

$$u_1 \to 0 \quad (2a)$$

$$u_2 \to u_2(x_2; t) \quad (2b)$$

$$\psi_1 \to \psi_1(x_2; t) \equiv \theta(x_2; t) \quad (2c)$$

where $\theta$ denotes the twist angle of the wing about its pitching axis (positive nose up).

In order to reduce the three-dimensional problem of the wing structure to an equivalent one-dimensional one, we will further postulate

$$\psi_2(x_1, x_2; t) = f_2(x_2; t) + x_1 g_2(x_2; t) \quad (3a)$$

$$u_3(x_1, x_2; t) = h(x_2; t) - (x_1 - x_0)\theta(x_2; t) \quad (3b)$$

Equation (3b) describes the vertical displacement of a wing of rigid cross sections where $h(x_2; t)$ denotes the plunging displacement of the wing cross sections measured at the elastic axis {positive upward and located at $x_1 = x_0\,[\equiv x_0(x_2)]$}. Based on Eqs. (2) and (3), Eq. (1) becomes

$$U_1 = x_3\theta(x_2; t) \quad (4a)$$

$$U_2 = u_2(x_2; t) + x_3(f_2 + x_1 g_2) \quad (4b)$$

$$U_3 = h(x_2; t) - (x_1 - x_0)\theta(x_2; t) \quad (4c)$$

Within the linearized elasticity theory, and in conjunction with Eq. (4), the strain components $e_{ij}$ result as

$$e_{11} = U_{1,1} = 0 \quad (5a)$$

$$e_{22} = U_{2,2} = u_{2,2} + x_3(f_{2,2} + \delta_1 x_1 g_{2,2}) \quad (5b)$$

$$\gamma_{12}(\equiv 2e_{12}) = U_{1,2} + U_{2,1} = x_3(\theta_{,2} + g_2) \quad (5c)$$

$$e_{33} = U_{3,3} = 0 \quad (5d)$$

$$\gamma_{13}(\equiv 2e_{13}) = U_{1,3} + U_{3,1} = 0 \quad (5e)$$

$$\gamma_{23}(\equiv 2e_{23}) = f_2 + x_1 g_2 + h_{,2} - x_1\theta_{,2} + (x_0\theta)_{,2} \quad (5f)$$

In Eq. (5) and in the forthcoming developments, $(\,)_{,i} \equiv \partial(\,)/\partial x_i$. Notice that a tracer $\delta_1$ has been included in the coefficient of $g_{2,2}$ of Eq. (5b) to identify the warping effect. $\delta_1$ takes the values 0 or 1, according to whether the free warping or warping restraint are implied, respectively.

It should be remarked that for

$$f_2 = -h_{,2} - (x_0\theta)_{,2} \quad (6a)$$

$$g_2 = \theta_{,2} \quad (6b)$$

the traditional Kirchhoff's model of wing structures[13-15] is deduced, according to which $\gamma_{13} = \gamma_{23} = 0$.

## Equations of Motion and Boundary Conditions

Hamilton's variational principle will be used to derive the equations of motion and the boundary conditions.[22] Accord-

ing to this principle, among all admissible displacements (paths) which fulfill the geometrical boundary conditions on $\Omega_u$ (i.e., $U_i = \underset{\sim}{U}_i$ on $\Omega_u$ where $\Omega = \Omega_u \cup \Omega_\sigma$ and $\Omega_u \cap \Omega_\sigma = \emptyset$, with $\Omega_\sigma$ being the complementary part of the body surface $\Omega$) and the conditions that $\delta U_i = 0$ at $t = t_0$ and $t = t_1$, where $t_0$ and $t_1$ denote the initial and final times of the motion, respectively, the actual one renders the functional

$$J \equiv \int_{t_0}^{t_1} (\mathcal{U} - \mathcal{K} + \mathcal{A})\, dt \tag{7}$$

stationary.

In Eq. (7), $\mathcal{U}$, $\mathcal{K}$, and $\mathcal{A}$ denote the strain energy, the kinetic energy, and the potential energy of the body and surface forces, respectively. From the stationary condition $\delta J = 0$, consistent with Eq. (7) and adopting the Einstein summation convention, we may easily obtain

$$\delta J = 0 = \int_{t_0}^{t_1} dt \left[ -\int_\tau \sigma_{ij}\delta U_{i,j}\, d\tau + \int_\tau \rho(\mathcal{H}_i - \ddot{U}_i)\delta U_i\, d\tau + \int_{\Omega\sigma} \underset{\sim}{\sigma}_i \delta U_i\, d\Omega \right] \tag{8}$$

Here, $\tau$ denotes the volume of the wing structure, $\mathcal{H}_i$ represents the $i$th component of the body force vector $\mathcal{H}$ (per unit mass), $\sigma_{ij}$ denote the components of the stress tensor, $\rho$ is the mass density, while the overdot denotes the time derivative. In addition, an undertilde affecting a quantity identifies a prescribed quantity while $\delta$ is the variation sign.

Having in view that

$$d\tau = dA\, dx_2 \tag{9}$$

where $A$ denotes the cross-sectional area of the wing, we may express

$$\int_\tau [\cdot]\, d\tau = \int_0^l dx_2 \int_A [\cdot]\, dA \tag{10}$$

where $2l$ denotes the total span of the wing.

Defining the generalized stress couples of order $(m, p)$ per unit span as[24]

$$T_{ij}^{(m,p)}(x_2) = \int_A \sigma_{ij} x_1^m x_3^p\, dA \tag{11}$$

having in view Eq. (10) and the representation [Eq.(4)] for $U_i$; taking in the first integral of Eq. (8) the variations of the displacement quantities and performing whenever possible integration by parts, one obtains

$$\begin{aligned}\int_\tau \sigma_{ij}\delta U_{i,j}\, d\tau = &-\int_0^l \{T_{22,2}^{(0,0)}\delta u_2 + [T_{22,2}^{(0,1)} - T_{23}^{(0,0)}]\delta f_2 \\ &+ [\delta_1 T_{22,2}^{(1,1)} - T_{12}^{(0,1)} - T_{23}^{(1,0)}]\delta g_2 + T_{23,2}^{(0,0)}\delta h \\ &+ [T_{12,2}^{(0,1)} - T_{23,2}^{(1,0)} + x_0 T_{23,2}^{(0,0)}]\delta\theta\}\, dx_2 + [T_{22}^{(0,0)}\delta u_2]_0^l \\ &+ [T_{22}^{(0,1)}\delta f_2]_0^l + [\delta_1 T_{22}^{(1,1)}\delta g_2]_0^l + [T_{23}^{(0,0)}\delta h]_0^l \\ &+ \{[T_{12}^{(0,1)} - T_{23}^{(1,0)} + T_{23}^{(0,0)} x_0]\delta\theta\}_0^l\end{aligned} \tag{12}$$

As a next step, the evaluation of the integral

$$\int_{\Omega_\sigma} \underset{\sim}{\sigma}_i \delta U_i\, d\Omega \tag{13}$$

has to be performed. To this end, it should be observed that for a cantilever wing its total external area can be represented as the reunion of partial areas as

$$\Omega = \Omega^+ \cup \Omega^- \cup \Omega^R \tag{14}$$

Here $\Omega^+$, $\Omega^-$, and $\Omega^R$ denote the upper surface, lower surface, and the right end cross-sectional area of the wing, respectively.

It may readily be seen that on $\Omega^+$ and $\Omega^-$ we have

$$\sigma_3^+ = \sigma_{33}^+ = P^+; \qquad \sigma_1^+ = \sigma_2^+ = 0 \tag{15}$$

so that on $\Omega^+ \cup \Omega^-$ it results

$$\underset{\sim}{\sigma}_3^+ - \underset{\sim}{\sigma}_3^- = P^+ - P^- = \Delta P \tag{16}$$

On $\Omega_R$ we have

$$\boldsymbol{\sigma}_n = \underset{\sim}{\sigma}_{12}\boldsymbol{i}_1 + \underset{\sim}{\sigma}_{22}\boldsymbol{i}_2 + \underset{\sim}{\sigma}_{23}\boldsymbol{i}_3 \tag{17}$$

where $\boldsymbol{i}_1$, $\boldsymbol{i}_2$, and $\boldsymbol{i}_3$ denote the unit vectors associated with the rectangular coordinates $x_1$, $x_2$, and $x_3$, respectively.

In light of Eqs. (14–17), Eq. (13) becomes

$$\begin{aligned}\int_{\Omega_\sigma} \underset{\sim}{\sigma}_i \delta U_i\, d\Omega = &\int_{\Omega^+\cup\Omega^-} \Delta P[\delta h - (x_1 - x_0)\delta\theta]\, d\Omega \\ &+ \int_{\Omega_R} \sigma_{21}\delta U_1(l)\, d\Omega + \int_{\Omega_R} \sigma_{22}\delta U_2(l)\, d\Omega \\ &+ \int_{\Omega_R} \sigma_{23}\delta U_3(\ell)\, d\Omega\end{aligned} \tag{18}$$

Defining

$$\begin{aligned}\mathcal{L}(x_2) &= \int_{\text{chord}} \Delta P\, dx_1 \\ \mathcal{T}(x_2) &= \int_{\text{chord}} \Delta P(x_1 - x_0)\, dx_1\end{aligned} \tag{19}$$

as the sectional lift and aerodynamic torque about the elastic axis per unit span, and in conjunction with Eqs. (14) and (19), Eq. (18) modifies as

$$\begin{aligned}\int_{\Omega_\sigma} \underset{\sim}{\sigma}_i \delta U_i\, d\Omega = &\int_0^l (\mathcal{L}\delta h + \mathcal{T}\delta\theta)\, dx_2 + T_{22}^{(0,0)}\delta u_2(l) \\ &+ T_{22}^{(0,1)}\delta f_2(l) + \delta_1 T_{22}^{(1,1)}\delta g_2(l) + T_{23}^{(0,0)}\delta h(l) \\ &+ [T_{12}^{(0,1)} - T_{23}^{(1,0)} + x_0(l)T_{23}^{(0,0)}]\delta\theta(l)\end{aligned} \tag{20}$$

Finally, to complete the derivation of the equations of motion, the evaluation of

$$\int_\tau \rho(\mathcal{H}_i - \ddot{U}_i)\delta U_i\, d\tau \tag{21}$$

has to be performed. Employment in Eq. (21) of Eqs. (4) and (10), and of the definitions[24]

$$\begin{bmatrix} F_i^{(m,p)}(x_2) \\ I^{(m,p)}(x_2) \end{bmatrix} = \int_A \rho \begin{bmatrix} \mathcal{H}_i \\ 1 \end{bmatrix} x_1^m x_3^p\, dA \tag{22}$$

for the generalized body forces and mass terms [of order $(m, p)$], respectively, Eq. (21) becomes

$$\int_\tau \rho(\mathcal{H}_i - \ddot{U}_i)\delta U_i \, d\tau = \int_0^l \{[F_2^{(0,0)} - I^{(0,0)}\ddot{u}_2 - I^{(0,1)}\ddot{f}_2 - \delta_1 I^{(1,1)}\ddot{g}_2]\delta u_2 + [F_2^{(0,1)} - I^{(0,1)}\ddot{u}_2 - I^{(0,2)}\ddot{f}_2 - \delta_1 I^{(1,2)}\ddot{g}_2]\delta f_2 + [F_2^{(1,1)} - I^{(1,1)}\ddot{u}_2 - I^{(1,2)}\ddot{f}_2 - \delta_1 I^{(2,2)}\ddot{g}_2]\delta g_2 + \{F_3^{(0,0)} - I^{(0,0)}\ddot{h} + [I^{(1,0)} - x_0 I^{(0,0)}]\ddot{\theta}\}\delta h + \{F_1^{(0,1)} - F_3^{(1,0)} + x_0 F_3^{(0,0)} - [I^{(0,2)} + I^{(2,0)} - 2x_0 I^{(1,0)} + x_0^2 I^{(0,0)}]\ddot{\theta} + [I^{(1,0)} - x_0 I^{(0,0)}]\ddot{h}\}\delta\theta\} \, dx_2 \quad (23)$$

Collecting in Eqs. (12), (20), and (23) the terms associated with the variations $\delta u_2$, $\delta f_2$, $\delta g_2$, $\delta h$, and $\delta\theta$, and having in view that these variations are independent and arbitrary, from the stationary condition $\delta J = 0$ [which concerns each instant belonging to the interval $(t_0, t_1)$], Eq. (8) yields

Equations of motion:

$$\delta u_2: \quad I^{(0,0)}\ddot{u}_2 + I^{(0,1)}\ddot{f}_2 + \delta_1 I^{(1,1)}\ddot{g}_2 - T_{22,2}^{(0,0)} - F_2^{(0,0)} = 0 \quad (24a)$$

$$\delta f_2: \quad I^{(0,1)}\ddot{u}_2 + I^{(0,2)}\ddot{f}_2 + \delta_1 I^{(1,2)}\ddot{g}_2 - T_{22,2}^{(0,1)} + T_{23}^{(0,0)} - F_2^{(0,1)} = 0 \quad (24b)$$

$$\delta g_2: \quad I^{(1,1)}\ddot{u}_2 + I^{(1,2)}\ddot{f}_2 + \delta_1 I^{(2,2)}\ddot{g}_2 - \delta_1 T_{22,2}^{(1,1)} + T_{12}^{(0,1)} + T_{23}^{(1,0)} - F_2^{(1,1)} = 0 \quad (24c)$$

$$\delta h: \quad I^{(0,0)}\ddot{h} - (I^{(1,0)} - x_0 I^{(0,0)})\ddot{\theta} - T_{23,2}^{(0,0)} - F_3^{(0,0)} - \mathcal{L} = 0 \quad (24d)$$

$$\delta\theta: \quad [I^{(0,2)} + I^{(2,0)} - 2x_0 I^{(1,0)} + x_0^2 I^{(0,0)}]\ddot{\theta} - [I^{(1,0)} - x_0 I^{(0,0)}]\ddot{h} - T_{12,2}^{(0,1)} + T_{23,2}^{(1,0)} - x_0 T_{23,2}^{(0,0)} - F_1^{(0,1)} + F_3^{(1,0)} - x_0 F_3^{(0,0)} + \mathcal{T} = 0 \quad (24e)$$

as well as the

Boundary conditions (BC):

At the root ($x_2 = 0$)

$$u_2 = \underset{\sim}{u}_2 \quad (25a)$$

$$f_2 = \underset{\sim}{f}_2 \quad (25b)$$

$$\delta_1 g_2 = \delta_1 \underset{\sim}{g}_2 \quad (25c)$$

$$h = \underset{\sim}{h} \quad (25d)$$

$$\theta = \underset{\sim}{\theta} \quad (25e)$$

and at the tip ($x_2 = l$)

$$\delta u_2: \quad T_{22}^{(0,0)} = \underset{\sim}{T}_{22}^{(0,0)} \quad (26a)$$

$$\delta f_2: \quad T_{22}^{(0,1)} = \underset{\sim}{T}_{22}^{(0,1)} \quad (26b)$$

$$\delta g_2: \quad \delta_1 T_{22}^{(1,1)} = \delta_1 \underset{\sim}{T}_{22}^{(1,1)} \quad (26c)$$

$$\delta h: \quad T_{23}^{(0,0)} = \underset{\sim}{T}_{23}^{(0,0)} \quad (26d)$$

$$\delta\theta: \quad T_{12}^{(0,1)} - T_{23}^{(1,0)} = \underset{\sim}{T}_{12}^{(0,1)} - \underset{\sim}{T}_{23}^{(1,0)} \quad (26e)$$

## Constitutive Equations

For a body whose material exhibits elastic symmetry with respect to the plane $x_3 = 0$ (monoclinic symmetry), the stress-strain relations are

$$\begin{bmatrix}\sigma_{11}\\ \sigma_{22}\\ \sigma_{12}\end{bmatrix} = \begin{bmatrix}\bar{Q}_{11} & \bar{Q}_{12} & \bar{Q}_{16}\\ \bar{Q}_{21} & \bar{Q}_{22} & \bar{Q}_{26}\\ \bar{Q}_{61} & \bar{Q}_{62} & \bar{Q}_{66}\end{bmatrix}\begin{Bmatrix}e_{11}\\ e_{22}\\ \gamma_{12}\end{Bmatrix} \quad (27)$$

$$\begin{bmatrix}\sigma_{13}\\ \sigma_{23}\end{bmatrix} = K^2\begin{bmatrix}Q_{44} & Q_{45}\\ Q_{54} & Q_{55}\end{bmatrix}\begin{Bmatrix}\gamma_{13}\\ \gamma_{23}\end{Bmatrix} \quad (28)$$

where $K^2$ is the transverse shear correction factor; $Q_{ij}$ and $\bar{Q}_{ij}$ are the elastic moduli and their reduced counterparts, respectively.

The governing equations for the wing structure are obtained by expressing in Eq. (24) the stress couples $T_{ij}^{(m,p)}$ in terms of the basic unknowns, by using the constitutive equations and Eq. (5). For example, $T_{22}^{(0,0)}$ can be expressed successively as

$$T_{22}^{(0,0)} = \int_A \sigma_{22} \, dA = \int_c dx_1 \int_H \sigma_{22} \, dx_3 = \int_c dx_1 \left[\sum_{k=1}^{n}\int_{z_{(k-1)}}^{z_{(k)}} \sigma_{22}^{(k)} \, dx_3\right] = \int_c dx_1 \left\{\sum_{k=1}^{n}\int_{z_{(k-1)}}^{z_{(k)}} [\bar{Q}_{21}^{(k)}e_{11} + \bar{Q}_{22}^{(k)}e_{22} + \bar{Q}_{26}^{(k)}\gamma_{12}] \, dx_3\right\} = \int_c dx_1 \left[\sum_{k=1}^{n}\int_{z_{(k-1)}}^{z_{(k)}} [\bar{Q}_{22}^{(k)}(u_{2,2} + x_3 f_{2,2} + \delta_1 x_1 x_3 g_{2,2}) + \bar{Q}_{26}^{(k)}x_3(\theta_{,2} + g_2)] \, dx_3\right] \quad (29)$$

where material properties are assumed to be piecewise constant across the thickness of the wing. In Eq. (29) $\int_c (\,) \, dx_1$ and $\int_H (\,) \, dx_3$ denote the integrals in the chordwise and thickness directions, respectively. For the sake of generality, in the forthcoming developments we will assume that the total thickness of the wing

$$H\left\{\equiv \sum_{k=1}^{n}[z_{(k)} - z_{(k-1)}]\right\}$$

has a variation in both chordwise and spanwise directions [i.e., that $H \equiv H(x_1, x_2)$]. Here, $z_{(k)}$ is the distance in the thickness direction from the reference plane to the top face of the $k$th layer, and $\bar{Q}_{ij}^{(k)}$ are the reduced orthotropic moduli of the $k$th layer. Using the definitions for the stiffness quantities given in Appendix A, the stress couple $T_{22}^{(0,0)}$ takes the form:

$$T_{22}^{(0,0)} = \bar{A}_{22}u_{2,2} + \bar{B}_{22}f_{2,2} + \delta_1\bar{\bar{B}}_{22}g_{2,2} + \bar{B}_{26}\theta_{,2} + \bar{B}_{26}g_2 \quad (30)$$

Similarly, the remaining stress couples in terms of the displacement quantities are

$$T_{22}^{(0,1)} = \bar{B}_{22}u_{2,2} + \bar{D}_{22}f_{2,2} + \delta_1\bar{\bar{D}}_{22}g_{2,2} + \bar{D}_{26}\theta_{,2} + \bar{D}_{26}g_2 \quad (31a)$$

$$T_{23}^{(0,0)} = \bar{A}_{55}f_2 + \bar{\bar{A}}_{55}g_2 + \bar{A}_{55}h_{,2} + \bar{A}_{55}(x_0\theta)_{,2} - \bar{\bar{A}}_{55}\theta_{,2} \quad (31b)$$

$$T_{22}^{(1,1)} = \bar{\bar{B}}_{22}u_{2,2} + \bar{\bar{D}}_{22}f_{2,2} + \delta_1\bar{\bar{D}}_{22}g_{2,2} + \bar{\bar{D}}_{26}\theta_{,2} + \bar{\bar{D}}_{26}g_2 \quad (31c)$$

$$T_{12}^{(0,1)} = \bar{B}_{62}u_{2,2} + \bar{D}_{62}f_{2,2} + \delta_1\bar{\bar{D}}_{62}g_{2,2} + \bar{D}_{66}\theta_{,2} + \bar{D}_{66}g_2 \quad (31d)$$

$$T_{23}^{(1,0)} = \bar{\bar{A}}_{55} f_2 + \bar{\bar{\bar{A}}}_{55} g_2 + \bar{\bar{A}}_{55} h_{,2} + \bar{\bar{A}}_{55}(x_0\theta)_{,2} - \bar{\bar{\bar{A}}}_{55}\theta_{,2} \tag{31e}$$

## Governing Equations

Replacement of Eqs. (30) and (31) in Eq. (24) results in the equations governing the motion of wing structures under the lift force $\mathcal{L}$ and the torque $\mathcal{T}$. These are

$$\delta u_2: \quad I^{(0,0)}\ddot{u}_2 + I^{(0,1)}\ddot{f}_2 + \delta_1 I^{(1,1)}\ddot{g}_2 - (\bar{A}_{22}u_{2,2} + \bar{B}_{22}f_{2,2} + \delta_1\bar{\bar{B}}_{22}g_{2,2} + \bar{B}_{26}\theta_{,2} + \bar{B}_{26}g_2)_{,2} - F_2^{(0,0)} = 0 \tag{32a}$$

$$\delta f_2: \quad I^{(0,2)}\ddot{f}_2 + I^{(0,1)}\ddot{u}_2 + \delta_1 I^{(1,2)}\ddot{g}_2 - (\bar{B}_{22}u_{2,2} + \bar{D}_{22}f_{2,2} + \delta_1\bar{\bar{D}}_{22}g_{2,2} + \bar{D}_{26}\theta_{,2} + \bar{D}_{26}g_2)_{,2} + [\bar{A}_{55}f_2 + \bar{\bar{A}}_{55}g_2 + \bar{A}_{55}h_{,2} + \bar{A}_{55}(x_0\theta)_{,2} - \bar{\bar{A}}_{55}\theta_{,2}] - F_2^{(0,1)} = 0 \tag{32b}$$

$$\delta g_2: \quad \delta_1 I^{(2,2)}\ddot{f}_2 + I^{(1,1)}\ddot{u}_2 + I^{(1,2)}g_2 - (\bar{\bar{B}}_{22}u_{2,2} + \bar{\bar{D}}_{22}f_{2,2} + \delta_1\bar{\bar{\bar{D}}}_{22}g_{2,2} + \bar{\bar{D}}_{26}\theta_{,2} + \bar{\bar{D}}_{26}g_2)_{,2} + (\bar{B}_{62}u_{2,2} + \bar{D}_{62}f_{2,2} + \delta_1\bar{\bar{D}}_{62}g_{2,2} + \bar{D}_{66}\theta_{,2} + \bar{D}_{66}g_2) + [\bar{\bar{A}}_{55}f_2 + \bar{\bar{\bar{A}}}_{55}g_2 + \bar{\bar{A}}_{55}h_{,2} + \bar{\bar{A}}_{55}(x_0\theta)_{,2} - \bar{\bar{\bar{A}}}_{55}\theta_{,2}] - F_2^{(1,1)} = 0 \tag{32c}$$

$$\delta h: \quad I^{(0,0)}\ddot{h} - [I^{(1,0)} - x_0 I^{(0,0)}]\ddot{\theta} - [\bar{A}_{55}f_2 + \bar{\bar{A}}_{55}g_2 + \bar{A}_{55}h_{,2} + \bar{A}_{55}(x_0\theta)_{,2} - \bar{\bar{A}}_{55}\theta_{,2}]_{,2} - F_3^{(0,0)} - \mathcal{L} = 0 \tag{32d}$$

$$\delta\theta: \quad [I^{(0,2)} + I^{(2,0)} - 2x_0 I^{(1,0)} + x_0^2 I^{(0,0)}]\ddot{\theta} - [I^{(1,0)} - x_0 I^{(0,0)}]\ddot{h} - (\bar{B}_{62}u_{2,2} + \bar{D}_{62}f_{2,2} + \delta_1\bar{\bar{D}}_{62}g_{2,2} + \bar{D}_{66}\theta_{,2} + \bar{D}_{66}g_2)_{,2} + [\bar{\bar{A}}_{55}f_2 + \bar{\bar{\bar{A}}}_{55}g_2 + \bar{\bar{A}}_{55}h_{,2} + \bar{\bar{A}}_{55}(x_0\theta)_{,2} - \bar{\bar{\bar{A}}}_{55}\theta_{,2}]_{,2} - x_0[\bar{A}_{55}f_2 + \bar{\bar{A}}_{55}g_2 + \bar{A}_{55}h_{,2} + \bar{A}_{55}(x_0\theta)_{,2} - \bar{\bar{A}}_{55}\theta_{,2}]_{,2} - F_1^{(0,1)} + F_3^{(1,0)} - x_0 F_3^{(0,0)} - \mathcal{T} = 0 \tag{32e}$$

The expressions of mass terms $I^{(m,p)}$ are displayed in Appendix A. Concerning the static boundary condition (at the wingtip) they can also be converted in terms of the basic unknowns.

## Alternative Form for the Aeroelastic Governing Equations

Equation (32) constitute a tenth-order system of five partial differential equations (PDEs) in terms of the basic unknown functions $u_2$, $f_2$, $g_2$, $h$, and $\theta$. However, this system of governing equations can be equivalently reduced to a system of four PDEs in terms of the unknowns $f_2$, $g_2$, $\theta$, and $h$, only. To this end we proceed to a simplification of Eq. (24a). Upon disregarding the influence of the in-plane component of body forces $F_2^{(0,0)}$, as well as of in-plane and rotatory inertia terms (i.e., terms $I^{(0,0)}\ddot{u}_2$, $I^{(0,1)}\ddot{f}_2$, and $I^{(1,1)}\ddot{g}_2$), Eq. (24a) can be expressed as

$$T_{22,2}^{(0,0)} = 0 \tag{33}$$

Integration of this equation yields

$$T_{22}^{(0,0)} = C(x_1) \tag{34}$$

where $C(x_1)$ is an arbitrary function of $x_1$. However, by virtue of the BC [Eq. (26a)] and upon postulating that there are no in-plane spanwise loads at the wingtip, we have

$$T_{22}^{(0,0)} = 0 \quad \text{at} \quad x_2 = l \tag{35}$$

Comparison of Eq. (34) with Eq. (35) yields

$$C(x_1) = 0 \tag{36}$$

By virtue of Eq. (30), used in conjunction with Eqs. (34) and (35), one obtains

$$\bar{A}_{22}u_{2,2} + \bar{B}_{22}f_{2,2} + \delta_1\bar{\bar{B}}_{22}g_{2,2} + \bar{B}_{26}\theta_{,2} + \bar{B}_{26}g_2 = 0 \tag{37}$$

From this equation it is possible to express $u_{2,2}$ as

$$u_{2,2} = -(1/\bar{A}_{22})(\bar{B}_{22}f_{2,2} + \delta_1\bar{\bar{B}}_{22}g_{2,2} + \bar{B}_{26}\theta_{,2} + \bar{B}_{26}g_2) \tag{38}$$

In conjunction with Eq. (38), eliminating $u_2$ from the system [Eq. (32)], the aeroelastic governing equations result in a system of only four PDEs in terms of the basic unknowns $f_2$, $g_2$, $h$, and $\theta$. Moreover, replacement of $u_{2,2}$ as expressed by Eq. (38) in the BCs results in only two sets of four boundary conditions expressed at $x_2 = 0$ and $x_2 = l$, respectively. The BCs which should be fulfilled at $x_2 = 0$ are, $f_2 = f_2$; $\delta_1 g_2 = \delta_1 g_2$; $h = h$; $\theta = \theta$. As concerns the BCs at $x_2 = l$, these will not be displayed here.

Consistent with this number of BCs, an eighth-order system of four PDEs governing the aeroelastic motion of a cantilevered wing is obtained.

Equation (32), or its transformed counterparts, can be applied to the study of a variety of aeroelastic phenomena of anisotropic, composite cantilevered swept-wing structures. However, within this article, only an assessment of the effects of transverse shear deformation and warping restraint upon the static aeroelastic response and divergence of a composite cantilevered swept wing will be given. To this end, a spanwise uniform rectangular swept wing composed of a transversely isotropic material is considered.

## Case Study: Uniform Rectangular Swept-Wing Model

Consider a swept (forward or backward) uniform rectangular wing with a straight elastic axis coinciding with the reference axis directed along the spanwise midchord line for which case $x_0 = 0$ (see Fig. 1). The wing is composed of a single transversely isotropic material whose plane of isotropy is parallel at each point to the reference plane of the wing. For such a material the nonzero elastic coefficients are[22]

$$\bar{Q}_{11} = \bar{Q}_{22} = \frac{E}{1 - \nu^2} \tag{39a}$$

$$\bar{Q}_{12} = \frac{E}{1 - \nu^2} \tag{39b}$$

$$\bar{Q}_{66} \equiv G_{12} = \frac{E}{2(1 + \nu)} \tag{39c}$$

$$Q_{44} = Q_{55} = G' \tag{39d}$$

In Eq. (39), $E$ and $\nu$ denote the ratio associated with the plane of isotropy, whereas $G_{12}$ denotes the tangential shear modulus. All geometric and structural properties are constant along the span, and the chordwise rigidity assumption yields constant values for the stiffness coefficients in the chordwise direction.

The static counterpart of the governing Eq. (32) considered in conjunction with Eq. (38), and with the fact that for the

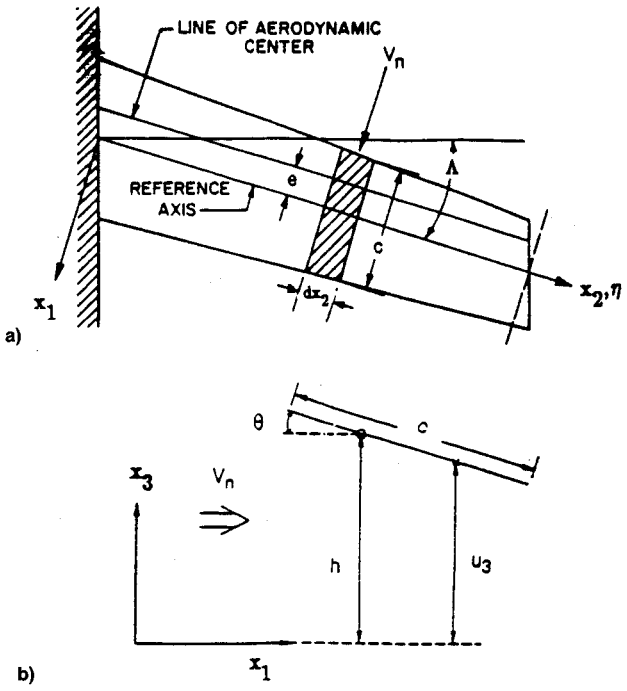


**Fig. 1 a) Geometry of a swept wing and b) the chordwise-rigid plate model.**

considered structural configuration the coupling stiffness terms $B_{ij}$ vanish, results in

$$\frac{R}{3(1-\nu)^2}\left(\frac{\bar{H}}{\mathrm{AR}}\right)^2 f_2^{*\prime\prime} - f_2^* - h^{*\prime} = 0 \tag{40a}$$

$$\left[\frac{R}{2(1+\nu)}\bar{H}^2 + 1\right] g_2^* + \left[\frac{R}{2(1+\nu)}\bar{H}^2 - 1\right]\theta^{*\prime} - \frac{R}{3(1-\nu^2)}\left(\frac{\bar{H}}{\mathrm{AR}}\right)^2 \delta_1 g_2^{*\prime\prime} = 0 \tag{40b}$$

$$f_2^{*\prime} + h^{*\prime\prime} + \frac{R}{6(1-\nu^2)}\frac{\bar{H}^2}{\mathrm{AR}} a_0 Q_n \theta^* - \frac{R}{3(1-\nu^2)}\left(\frac{\bar{H}}{\mathrm{AR}}\right)^2 a_0 \tan\Lambda Q_n h^{*\prime} = -\frac{R}{6(1-\nu^2)}\frac{\bar{H}^2}{\mathrm{AR}} a_0 \bar{\alpha}_0 Q_n \tag{40c}$$

$$\left[\frac{R}{2(1+\nu)}\bar{H}^2 - 1\right] g_2^{*\prime} + \left[\frac{R}{2(1+\nu)}\bar{H}^2 + 1\right]\theta^{*\prime} + 2\frac{R}{1-\nu^2}\frac{\bar{H}^2}{\mathrm{AR}} a_0 \bar{e} Q_n \theta^* - 4\frac{R}{1-\nu^2}\left(\frac{\bar{H}}{\mathrm{AR}}\right)^2 a_0 \bar{e} Q_n \tan\Lambda h^{*\prime} = -2\frac{R}{1-\nu^2}\frac{\bar{H}^2}{\mathrm{AR}}(a_0 \bar{e}\bar{\bar{\alpha}}_0 + C_{\mathrm{mac}})Q_n \tag{40d}$$

whereas the associated boundary conditions are

at $\eta = 0$

$$f_2^* = g_2^* = h^* = \theta^* = 0 \tag{41}$$

and at $\eta = 1$

$$f_2^{*\prime} = g_2^{*\prime} = f_2^* + h^{*\prime} = \left[\frac{R}{2(1+\nu)}\bar{H}^2 - 1\right] g_2^* + \left[\frac{R}{2(1+\nu)}\bar{H}^2 + 1\right]\theta^{*\prime} = 0 \tag{42}$$

In the above equations the starred quantities are defined as

$$\begin{aligned} h^* &= h/c \\ \theta^* &= \theta \\ f_2^* &= \mathrm{AR}\, f_2/2 \\ g_2^* &= l g_2 \end{aligned} \tag{43}$$

while the primes indicate differentiation with respect to the nondimensional spanwise coordinate $\eta$. In addition, $Q_n \equiv q_n c l^3/\bar{D}_{22}$ is the normalized dynamic pressure; while $\bar{\alpha}_0$ and $\bar{\bar{\alpha}}_0$ are defined respectively as

$$\begin{aligned} \bar{\alpha}_0 &= \alpha_0 - \alpha_{\mathrm{corr}} \\ \bar{\bar{\alpha}}_0 &= \alpha_0 - \alpha_{\mathrm{corr}}\, \mathrm{d}/e \end{aligned} \tag{44}$$

where $\alpha_{\mathrm{corr}}$ represents a correction to the rigid angle of attack $\alpha_0$ due to the wing load factor $N$ defined as

$$N = \frac{2l}{W} c q_n a_0 \int_0^1 \alpha_{\mathrm{eff}}\, \mathrm{d}\eta = \frac{2l}{W} c q_n a_0 \alpha_{\mathrm{corr}} \tag{45}$$

where

$$\alpha_{\mathrm{eff}} = \alpha_0 + \theta^* - \frac{2\tan\Lambda}{\mathrm{AR}} h^{*\prime} \tag{46}$$

Equation (46) expresses the effect of bending deformation on the effective angle of attack $\alpha_{\mathrm{eff}}$, i.e., amplification for a swept-forward wing ($\Lambda < 0$), and attenuation for a swept-back wing ($\Lambda > 0$). The determination of $\alpha_{\mathrm{eff}}$ in Eq. (46) requires the solution of the system of Eqs. (39–45). Initially, by solving the system of Eq. (40) in conjunction with the boundary conditions [Eqs. (41) and (42)], based on a solution with a zero load factor is obtained. Based on this initial solution, $N$ is computed from Eq. (45) which, in turn, is substituted back in Eqs. (40) and (45). Upon repeating this iterative procedure, the solution to the static aeroelastic problem is obtained when a convergence criterion for $N$ is satisfied. The results obtained for $\theta^*$ and $h^{*\prime}$ give the spanwise distribution of the effective angle of attack [Eq. (46)] which in turn, yields the static aeroelastic load distribution $\mathcal{L} = q_n c \alpha_0 \alpha_{\mathrm{eff}}$. Implicit in the above solution is the effect of transverse shear deformation quantified by the parameter $R = E/G'$. A zero value for $R$ corresponds to a structure featuring an infinite rigidity in transverse shear ($G' \to \infty$), which is consistent with Kirchhoff's model.

As a further reduction, $f_2^*$ and $g_2^*$ can be eliminated from the system of Eqs. (40–42) to result in an eighth-order system of two coupled ODEs in $h^*$ and $\theta^*$ which requires the prescription of four boundary conditions at each end. The resulting system of governing equations is

$$h^{*\prime\prime\prime\prime} - m_4 R Q_n h^{*\prime\prime} + m_3 R Q_n \theta^{*\prime\prime} + m_{14} Q_n h^{*\prime} - m_{13} Q_n \theta^* = m_{15} \tag{47a}$$

$$\theta^{*\prime\prime\prime\prime} - \frac{(4m_{12} - m_6 R Q_n)}{m_2 R + 1}\theta^{*\prime\prime} - m_{16} Q_n \theta^* + m_{17} Q_n h^{*\prime} - \frac{m_7}{m_2 R + 1} R Q_n h^{*\prime\prime} = m_{18} + m_{19} \tag{47b}$$

with the boundary conditions

at the root, $\eta = 0$

$$m_1 R h^{*'''} - m_1 m_4 R^2 Q_n h^{*''} + m_1 m_3 R^2 Q_n \theta^{*'} + h^{*'} = 0 \tag{48a}$$

$$m_1 R(m_2 R + 1)\theta^{*'''} + [(m_2 R - 1)^2 + m_1 m_6 R^2 Q_n]\theta^{*'} - m_1 m_7 R^2 Q_n h^{*''} = 0 \tag{48b}$$

$$h^* = 0 \tag{48c}$$

$$\theta^* = 0 \tag{48d}$$

at the tip, $\eta = 1$

$$h^{*''} + m_3 R Q_n \theta^* - m_4 R Q_n h^{*'} = -m_5 R \tag{49a}$$

$$(m_2 R + 1)\theta^{*''} + m_6 R Q_n \theta^* - m_7 R Q_n h^{*'} = -(m_8 + m_9)R \tag{49b}$$

$$h^{*'''} - m_4 R Q_n h^{*''} + m_3 R Q_n \theta^{*'} = 0 \tag{49c}$$

$$(m_2 R + 1)\theta^{*'''} - (4m_{12} - m_6 R Q_n)\theta^{*'} - m_7 R Q_n h^{*''} = 0 \tag{49d}$$

The coefficients intervening in the above equations are displayed in Appendix B.

In addition to transverse shear, the above system of equations and the associated boundary conditions incorporate the warping restraint effect. For a free warping model, Eq. (47a) remains the same and Eq. (48b) should be replaced by

$$(m_2 R + 1)\theta^{*''} + m_6 R Q_n \theta^* - m_7 R Q_n h^{*'} = -(m_8 + m_9)R \tag{50}$$

As to the associated boundary conditions, Eq. (49d) should be discarded, and Eq. (48b) should be replaced by

$$\theta^{*'} = 0 \quad \text{at} \quad \eta = 1 \tag{51}$$

It is also readily seen that due to the considered type of anisotropy considered herein, the bending-twist coupling is of aerodynamic nature only.

## Solution Methodology

The system of Eq. (47) in conjunction with BCs, Eqs. (48) and (49), can be solved for its eigenvalues and eigenmodes by the exact Laplace integral transform method *LT*. This technique transforms the eighth-order system [Eq. (47)] to a linear algebraic system of equations expressed formally as

$$\begin{bmatrix} A(s) & B(s) \\ C(s) & D(s) \end{bmatrix} \begin{bmatrix} \hat{h}(s) \\ \hat{\theta}(s) \end{bmatrix} = \begin{bmatrix} b_1 \\ b_2 \end{bmatrix} \tag{52}$$

where $\hat{h}(s) = LT[h^*(\eta)]$ and $\hat{\theta}(s) = LT(\theta^*(\eta)]$ are the Laplace transforms of $h^*$ and $\theta^*$, respectively. The terms of the determinant in Eq. (52), $A, \ldots, D$ are polynomials in $s$ whose coefficients are combinations of the constants defined in Appendix B as well as of the four unknown functions evaluated at the root ($\eta = 0$), namely $h^{*'}(0)$, $h^{*''}(0)$, $\theta^{*'}(0)$, and $\theta^{*''}(0)$. These quantities result from the application of the root boundary conditions [Eq. (48)] in the Laplace transformation process of the derivatives of $h^*$ and $\theta^*$. Solving Eq. (52) for $\hat{h}(s)$ and $\hat{\theta}(s)$ and taking their inverse Laplace transforms, the spanwise distribution of the mode shapes can be obtained as

$$\begin{aligned} h^*(\eta) &= H_1(\eta)h^{*'}(0) + H_2(\eta)h^{*''}(0) + H_3(\eta)\theta^{*'}(0) \\ &\quad + H_4(\eta)\theta^{*''}(0) + F_H(\eta) \\ \theta^*(\eta) &= T_1(\eta)h^{*'}(0) + T_2(\eta)h^{*''}(0) + T_3(\eta)\theta^{*'}(0) \\ &\quad + T_4(\eta)\theta^{*''}(0) + F_T(\eta) \end{aligned} \tag{53}$$

where the spanwise functions $H_i(\eta)$ and $T_i(\eta)$ ($i = \overline{1,4}$) depend on the parameters $R$, $Q_n$, AR, $\bar{H}$, $\nu$, $a_0$, $\bar{e}$, and $\Lambda$, whereas in addition to these parameters the functions $F_H(\eta)$ and $F_T(\eta)$ depend also on $\alpha_0$, $C_{mac}$, $d/e$, and $N$.

In order to determine the four unknown quantities in Eq. (53) we enforce the remaining four boundary conditions at the tip [Eq. (49)], yielding a linear system of equations for the four unknowns

$$AX = \boldsymbol{B} \tag{54}$$

where $X = [h^{*'}(0), h^{*''}(0), \theta^{*'}(0), \theta^{*''}(0)]^T$, $\boldsymbol{B}$ is a $4 \times 1$ vector containing linear combinations of $F_H$, $F_T$, and their spanwise derivatives evaluated at $\eta = 1$. The elements of the $4 \times 4$ matrix $A$ are a set of linear combinations of $H_i$, $T_i$, ($i = \overline{1,4}$), and their spanwise derivatives are evaluated at $\eta = 1$.

The lowest value of $Q_n$ for which $\det[A] = 0$ corresponds to the critical (divergence) dynamic pressure. In the subcritical flight range the solution of Eq. (52) yields the four unknown quantities needed for the determination of the mode shapes in Eq. (53). In turn, these mode shapes, when substituted in Eq. (46), will supply the static aeroelastic load distribution on a swept wing in the subcritical range. A detailed study of the combined and separate effects of transverse shear deformation and warping restraint upon divergence and load distribution is given below. Although restricted in the numerical illustrations to a special case, this method is quite versatile and can be applied to the most general case furnished by Eq. (32). Note that the above methodology is applied to the system with warping restraint effect. In similar fashion it can also be applied to the system with free warping exhibiting only three unknowns in this case, namely, $h^{*'}(0)$, $h^{*''}(0)$, and $\theta^{*'}(0)$.

## Numerical Illustrations

Several cases related to a rectangular swept-wing configuration of various aspect ratios with uniform cross sections are considered. Throughout the numerical illustrations the following parameters are prescribed: $C_{mac} = d = 0$, $\bar{e} = \bar{H} = 0.1$, $\nu = 0.25$, $\alpha_0 = 5$ deg, and $\alpha_0 = 2\pi/[1 + (4/\text{AR})\cos\Lambda]$. Here, we consider the transverse shear correction factor $K^2$ to be unity. The effects of transverse shear flexibilities will be reflected by the range of values from 0 to 100 assigned to $R$ ($\equiv E/G'$); $R = 0$ yielding the classical results based on Kirchhoff's hypothesis, and $R = 100$ corresponding to a rather high flexibility degree in transverse shear. The warping restraint and free warping effects will result from two separate sets of calculations (depending on whether $\delta_1$ takes on the value 1 or 0, respectively). In the case of warping restraint the order of the governing equations is eight, requiring fulfillment of four boundary conditions at each end of the wing. In the free warping case, the order is reduced by two, requiring fulfillment of only three boundary conditions at each end. Hence, in each case, the calculation of the mode shapes requires solving a separate system of equations.

The onset of static aeroelastic instability (divergence) corresponds to the lowest value of $\bar{Q}_n$ rendering zero the determinant of $A$. Three sets of results are obtained for the normalized divergence dynamic pressure $\bar{Q}_n$ as a function of $R$ for three forward sweep angles $\Lambda = -20$ deg, $-40$ deg, $-60$ deg. The warping restraint effect is implicit in these results. As expected, the wing with a higher forward-sweep angle becomes unstable at a lower dynamic pressure. The critical values of $\bar{Q}_n$ exhibit small variations over the entire range of $R$ including $R = 0$, pertinent to the classical theory; the maximum change being 6% for $\Lambda = -20$ deg, 3.5% for $\Lambda = -40$ deg, and 2% for $\Lambda = -60$ deg. In this case the effect of transverse shear deformation upon divergence is a higher order correction to the classical results. The reason for this weak effect stems from the fact that, at the onset of instability, the order of magnitude of the elements of the determinant of

the system [Eq. (54)], which contain the mode shapes and their derivatives evaluated at $\eta = 1$, becomes very high (infinite) and even higher for larger forward-sweep angles. Hence, the effect of a finite variation of $R$ on the order of magnitude of these elements is a higher-order effect, and much higher for larger forward-sweep angles. However, in the subcritical range, the magnitudes of the mode shapes and their derivatives are finite. Consequently, the effect of $R$ on these mode shapes should be more pronounced. Indeed, this can be seen in Fig. 2 where the effect of $R$ on the spanwise distribution of $\alpha_{\text{eff}}/\alpha_0$ is quite substantial. Two sets of results are shown, each corresponding to two sweep angles ($\Lambda = \pm 20$ deg), with $R$ varying from 0 to 100 with an increment of 10 in each case. Here, AR = 6 and the flight dynamic pressure is 75% of its critical value. Note that the distributions corresponding to $R = 0$ represent classical results. It is clear from these results how extensive the amplification effect of transverse shear deformation is on the static aeroelastic load distribution for a

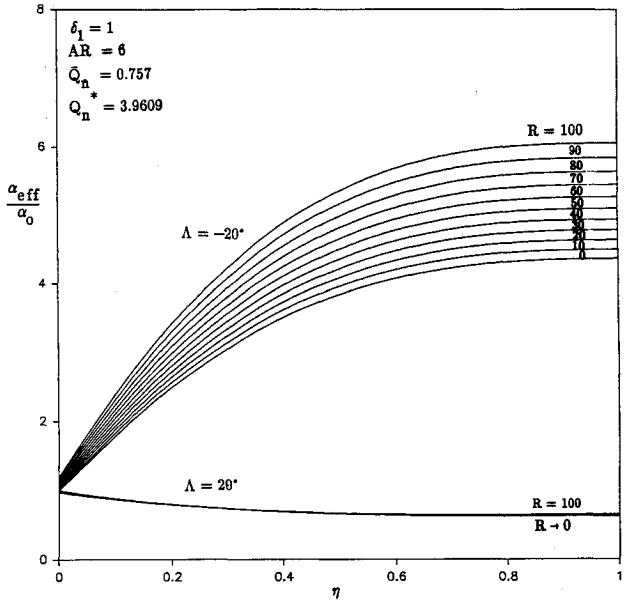


**Fig. 2 Spanwise distribution of the normalized effective angle of attack for $\Lambda = \pm 20$ deg and $E/G' = 10n$; $n = 0, 1, \ldots 10$, including WR effects.**

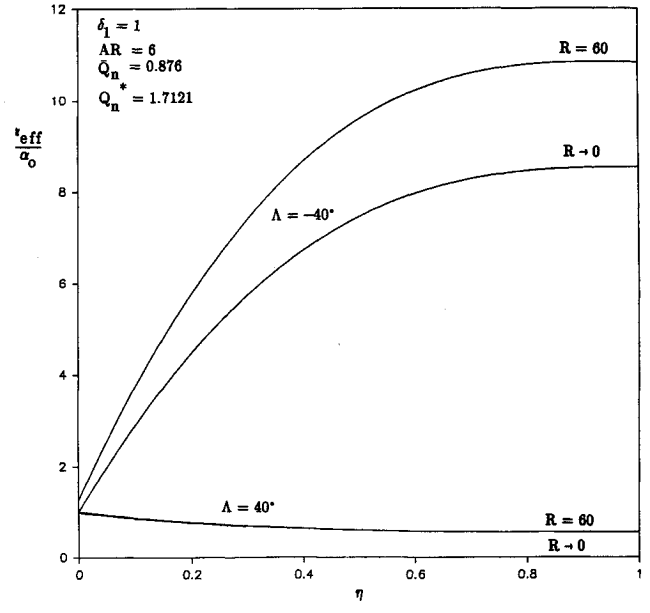


**Fig. 3 Spanwise distribution of the normalized effective angle of attack for the classical ($E/G' \to 0$) and TSD ($E/G' = 60$), including WR effects for $\Lambda = \pm 40$ deg.**

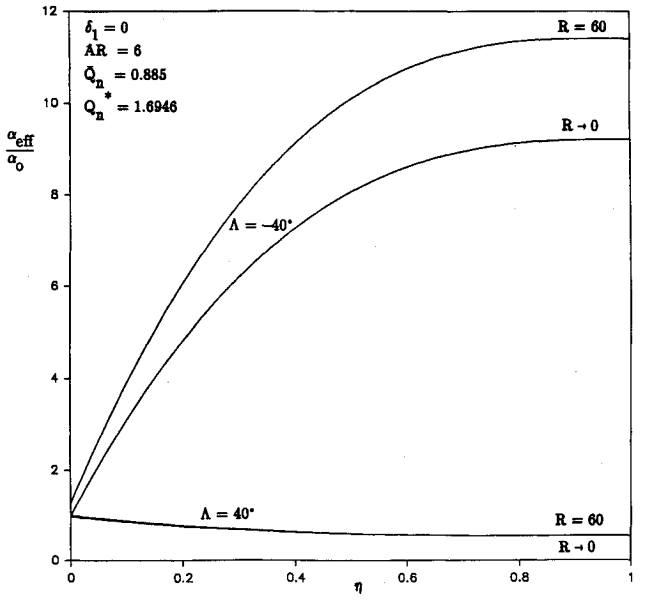


**Fig. 4 Spanwise distribution of the normalized effective angle of attack for the classical ($E/G' \to 0$) and TSD ($E/G' = 60$), excluding WR effects (FW) for $\Lambda = \pm 40$ deg.**

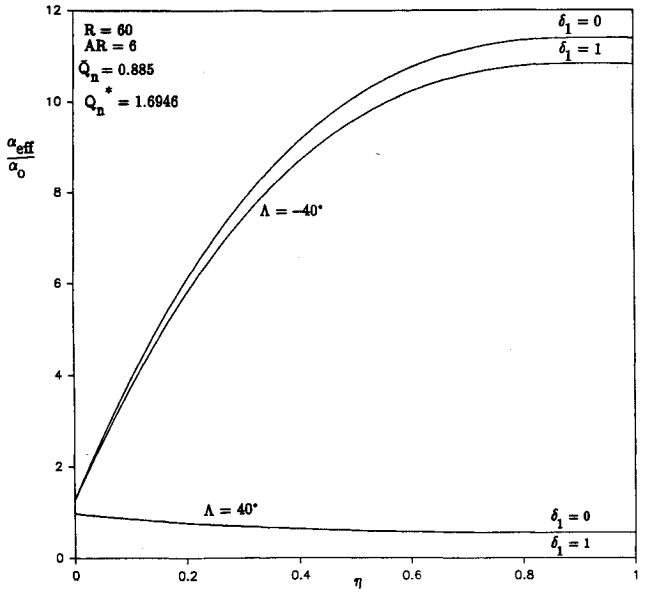


**Fig. 5 Warping restraint and free warping effects on the spanwise distribution of the normalized effective angle of attack for $E/G' = 60$ and $\Lambda = \pm 40$ deg.**

swept-forward wing. The comparison between the classical result ($R = 0$) and that for $R = 100$ yields an underestimation of the load distribution predicted by the classical theory by as much as 25%. It is obvious that we can no longer consider the effect of $R$ as a higher-order correction to the classical results, as was the case for the divergence calculations. However, for a swept-back wing the effect of $R$ is very small, and in this case the classical theory can be applied with enough confidence. Implicit in these results is the warping restraint effect. Here, we note that the combined effect of TSD and WR is to amplify the static load distribution more than what the classical theory predicts. However, in order to make a contrast between the warping restraint and free warping effects upon the static aeroelastic load distribution in the presence of transverse shear deformation, a swept-forward ($\Lambda = -40$ deg) and a swept-back ($\Lambda = 40$ deg) wing of AR = 6 in the subcritical flight range are considered. The spanwise distributions of $\alpha_{\text{eff}}/\alpha_0$ are generated for both warping restraint and free warping models and are displayed in Figs. 3

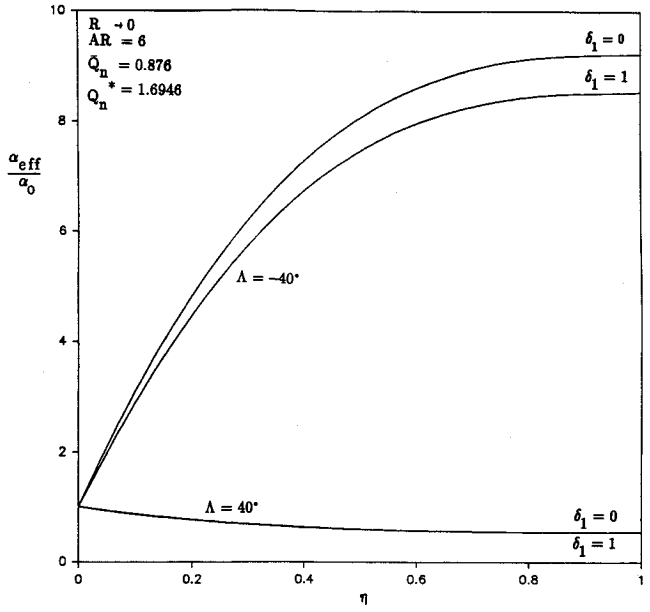


**Fig. 6 Warping restraint and free warping effects on the spanwise distribution of the normalized effective angle of attack within the framework of classical theory ($E/G' \to 0$) and for $\Lambda = \pm 40$ deg.**

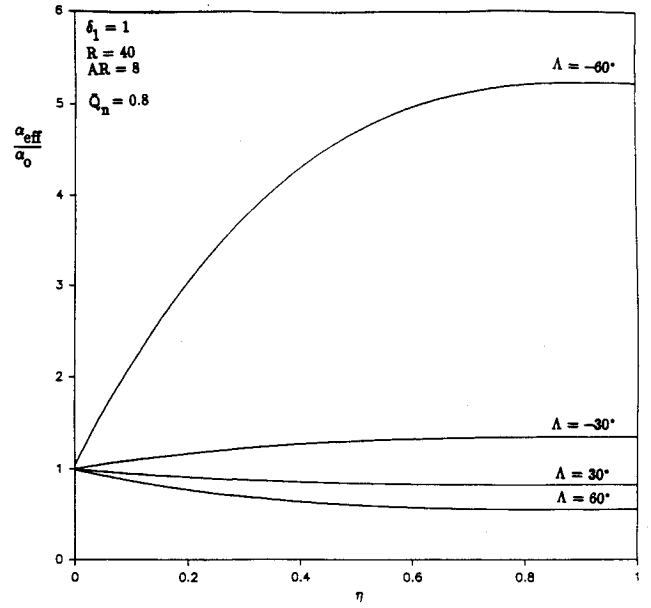


**Fig. 7 Spanwise distribution of $\alpha_{eff}/\alpha_0$ for wing sweeps $\Lambda = \pm 30$ deg and $\Lambda = \pm 60$ deg, including TSD and WR effects.**

and 4, respectively. In Fig. 3, the discrepancy between the classical results ($R = 0$) and the results for $R = 60$ is about 20% for $\Lambda = -40$ deg, and in the case of the free-warping model, Fig. 4, the discrepancy between similar results is slightly larger than that for the warping restraint model. To further evaluate the difference between the WR and FW models for a given $R$, Figs. 5 and 6 present such comparisons for $R = 60$ and $R = 0$, respectively. In comparison with the warping restraint model, the free warping model slightly overestimates the aeroelastic loads (5–7%) for $\Lambda = -40$ deg; both models yielding virtually the same result for $\Lambda = 40$ deg. Here, we note that the combined effects of TSD and FW tend to amplify the load distribution more than in the case of WR. Therefore, the exclusion of the WR effect yields a conservative estimate of the onset of static instability. Finally, forward sweep is found to have a profound impact on the static load distribution as shown in Fig. 7 when both TSD and WR effects are included. In passing, we must underline the fact that the amplification ratio measured in terms of $\alpha_{eff}/\alpha_0$ is shown to be relatively large in all above results (Figs. 2–7) due to the relatively chosen high subcritical flight speed range.

## Conclusions

A general formulation of aeroelastic equations for composite cantilevered swept-wing structures based on the first-order transverse shear deformation theory has been presented. The theory which is suitable for parametric studies represents a significant departure from the existing ones in that it incorporates a number of effects in the structural model which have not been considered up to this time. The previously derived models of wing-structures (as e.g., the ones in Refs. 4, 12, and 13) can be easily obtained by simple specialization of the present theory. In this work, a study of the effects of transverse shear deformation and warping restraint upon the static aeroelastic behavior of a uniform swept wing constructed from a transversely isotropic material is performed. Underestimated by the classical theory (infinite rigidity in transverse shear and free warping), these two effects, in a separate or coupled presence, yield a significant amplification of the aeroelastic load distribution for a swept-forward wing. These effects, however, only slightly alter the results of the aerodynamic load distribution for a swept-back wing, or the critical dynamic pressure for a swept-forward wing, obtained by the classical theory.

A subsequent study of the implications of these effects on other static and dynamic aeroelastic problems is underway.

## Appendix A

Expressions of the rigidity quantities and mass terms

$$[\bar{A}_{ij}(x_2), \bar{\bar{A}}_{ij}(x_2), \bar{\bar{\bar{A}}}_{ij}(x_2)] = \int_c A_{ij}(1, x_1, x_1^2)\, dx_1 \quad \text{(A1a)}$$

$$[\bar{B}_{ij}(x_2), \bar{\bar{B}}_{ij}(x_2), \bar{\bar{\bar{B}}}_{ij}(x_2)] = \int_c B_{ij}(1, x_1, x_1^2)\, dx_1 \quad \text{(A1b)}$$

$$[\bar{D}_{ij}(x_2), \bar{\bar{D}}_{ij}(x_2), \bar{\bar{\bar{D}}}_{ij}(x_2)] = \int_c D_{ij}(1, x_1, x_1^2)\, dx_1 \quad \text{(A1c)}$$

where

$$[A_{ij}(x_1, x_2), B_{ij}(x_1, x_2), D_{ij}(x_1, x_2)] \equiv \sum_{k=1}^{n} \int_{z_{(k-1)}}^{z_{(k)}} \bar{Q}_{ij}(1, x_3, x_3^2)\, dx_3 \quad \text{(A2)}$$

denote the stretching, bending-stretching and bending stiffness quantities, respectively.

A more explicit form of expressions Eq. (A2) is

$$\begin{bmatrix} A_{ij}(x_1, x_2) \\ B_{ij}(x_1, x_2) \\ D_{ij}(x_1, x_2) \end{bmatrix} = \sum_{k=1}^{n} \bar{Q}_{ij}^{(k)} \begin{bmatrix} z_{(k)} - z_{(k-1)} \\ \frac{1}{2}[z_{(k)}^2 - z_{(k-1)}^2] \\ \frac{1}{3}[z_{(k)}^3 - z_{(k-1)}^3] \end{bmatrix} \quad \text{(A3)}$$

while

$$A_{55}(x_1, x_2) = K^2 \sum_{k=1}^{n} Q_{55}^{(k)} [z_{(k)} - z_{(k-1)}] \quad \text{(A4)}$$

The mass terms $I^{(m,p)}$ defined in Eq. (22) can be expressed as

$$I^{(m,p)}(x_2) = \int_c x_1^m M_{p+1}\, dx_1 \quad \text{(A5)}$$

where

$$M_p = \frac{1}{p} \sum_{k=1}^{n} \rho_{(k)} [z_{(k)}^p - z_{(k-1)}^p] \quad \text{(A6)}$$

$\rho_{(k)}$ denoting the mass density of the $k$th layer.

## Appendix B

Coefficients intervening in Eqs. (47–49)

$$m_1 = \frac{(\bar{H}/\mathrm{AR})^2}{3(1-\nu^2)} \tag{B1a}$$

$$m_2 = \frac{\bar{H}^2}{2(1+\nu)} \tag{B1b}$$

$$m_3 = \tfrac{1}{2} m_1 a_0 \,\mathrm{AR} \tag{B1c}$$

$$m_4 = m_1 a_0 \tan\Lambda \tag{B1d}$$

$$m_5 = \tfrac{1}{2} m_1 a_0 \bar{\alpha}_0 \,\mathrm{AR}\, Q_n \tag{B1e}$$

$$m_6 = \frac{2a_0\bar{e}}{1-\nu^2}\frac{\bar{H}^2}{\mathrm{AR}} \tag{B1f}$$

$$m_7 = \frac{2\tan\Lambda}{\mathrm{AR}} m_6 \tag{B1g}$$

$$m_8 = m_6 Q_n \bar{\alpha}_0 \tag{B1h}$$

$$m_9 = \frac{2C_{\mathrm{mac}} Q_n}{1-\nu^2}\frac{\bar{H}^2}{\mathrm{AR}} \tag{B1i}$$

$$m_{1j} = \frac{m_j}{m_1},\ j = (\overline{2,9}) \tag{B1j}$$

## Acknowledgments

The authors extend their grateful appreciation to Ohseop Song for the useful technical discussions. G. Karpouzian expresses his gratitude to the Naval Academy Research Council (ONR) for the support provided to finalize this work.

## References

[1]Krone, N. J., Jr., "Divergence Elimination with Advanced Composites," AIAA Paper 75-1009, Aug. 1975.

[2]Weisshaar, T. A., "Aeroelastic Stability and Performance Characteristics of Aircraft with Advanced Composite Sweptforward Wing Structures," Air Force Flight Dynamics Lab. TR-78-116, Sept. 1978.

[3]Weisshaar, T. A., "Forward Swept Wing, Static Aeroelasticity," Air Force Flight Dynamics Lab. TR-3087, June 1979.

[4]Weisshaar, T. A., "Divergence of Forward Swept Composite Wings," *Journal of Aircraft*, Vol. 17, No. 6, 1980, pp. 442–448.

[5]Weisshaar, T. A., "Aeroelastic Tailoring of Forward Swept Composite Wings," *Journal of Aircraft*, Vol. 18, No. 8, 1981, pp. 669–676.

[6]Niblett, L. T., "Divergence and Flutter of Swept-Forward Wings with Cross-Flexibilities," Royal Aircraft Establishment TR-80047, April 1980.

[7]Sherrer, V. C., Hertz, T. J., and Shirk, M. H., "Wind Tunnel Demonstration of Aeroelastic Tailoring Applied to Forward Swept Wings," *Journal of Aircraft*, Vol. 18, No. 11, 1981, pp. 976–983.

[8]Lehman, L. L., "A Hybrid State Vector Approach to Aeroelastic Analysis," *AIAA Journal*, Vol. 20, No. 10, 1982, pp. 1442–1449.

[9]Hertz, T. J., Shirk, M. H., Ricketts, R. H., and Weisshaar, T. A., "On the Track of Practical Forward-Swept Wings," *Astronautics and Aeronautics*, Vol. 20, Jan. 1982, pp. 40–52.

[10]Hollowell, S. J., and Dugundji, J., "Aeroelastic Flutter and Divergence of Stiffness Coupled, Graphite/Epoxy, Cantilevered Plates," AIAA Paper 82-0722, May 1982; see also *Journal of Aircraft*, Vol. 21, No. 1, 1984, pp. 69–76.

[11]Oyibo, G. A., "Genetic Approach to Determine Optimum Aeroelastic Characteristics for Composite Forward-Swept-Wing Aircraft," *AIAA Journal*, Vol. 22, No. 1, 1984, pp. 117–123.

[12]Lottati, I., "Flutter and Divergence Aeroelastic Characteristics for Composite Forward Swept Cantilevered Wing," *Journal of Aircraft*, Vol. 22, No. 11, 1985, pp. 1001–1007.

[13]Librescu, L., and Simovich, J., "General Formulation for the Aeroelastic Divergence of Composite Swept-Forward Wing Structures," *Journal of Aircraft*, Vol. 25, No. 4, 1988, pp. 364–371.

[14]Librescu, L., and Khdeir, A. A., "Aeroelastic Divergence of Sweptforward Composite Wings Including Warping Restraint Effect," *AIAA Journal*, Vol. 26, No. 11, 1988, pp. 1373–1377.

[15]Librescu, L., and Thangjitham, S., "Analytical Studies on Static Aeroelastic Behavior of Forward-Swept Composite Wing Structures," *Journal of Aircraft*, Vol. 28, No. 2, 1990, pp. 151–157.

[16]Crawley, E. F., and Dugundji, J., "Frequency Determination and Non-Dimensionalization for Composite Cantilever Plates," *Journal of Sound and Vibration*, Vol. 72, No. 1, 1980, pp. 1–10.

[17]Bauchau, O. A., Coffenberry, B. S., and Rehfield, L. W., "Composite Box Beam Analysis: Theory and Experiments," *Journal of Reinforced Plastics and Composites*, Vol. 6, Jan. 1987, pp. 25–34.

[18]Oyibo, G. A., "Some Implications of Warping Restraint on the Behavior of Composite Anisotropic Beams," *Journal of Aircraft*, Vol. 26, No. 2, 1989, pp. 187–189.

[19]Oyibo, G. A., and Bentson, J., "Exact Solutions to the Oscillations of Composite Aircraft Wings with Warping Constraint and Elastic Coupling," *AIAA Journal*, Vol. 28, No. 6, 1990, pp. 1075–1081.

[20]Thangjitham, S., and Librescu, L., "Free Vibration Characteristics of Anisotropic Composite Wing Structures," AIAA Paper 91-1185, April 1991.

[21]Petre, A., Stanescu, C., and Librescu, L., "Aeroelastic Divergence of Multicell Wings Taking Their Fixing Restraints into Account," *Revue de Mecanique Appliqueé*, Vol. 19, No. 6, 1961, pp. 689–698.

[22]Librescu, L., *Elastostatics and Kinetics of Anisotropic and Heterogeneous Shell-Type Structures*, Noordhoff International Publishing, Leyden, The Netherlands, 1975.

[23]Noor, A. K., and Burton, W. S., "Assessment of Shear Deformation for Multilayered Composite Plates," *Appl. Mech. Rev.*, Vol. 42, No. 1, 1989, pp. 1–12.

[24]Dökmeci, M. C., "A General Theory of Elastic Beams," *International Journal of Solids and Structures*, Vol. 8, 1972, pp. 1205–1222.